

# Ultrafast Measurements of Excited State Intramolecular Proton Transfer (ESIPT) in Room Temperature Solutions of 3-Hydroxyflavone and Derivatives

Simon Ameer-Beg, Stuart M. Ormson, and Robert G. Brown\*

Centre for Photochemistry, University of Central Lancashire, Preston, Lancs PR1 2HE, UK

Pavel Matousek and Mike Towrie

Central Laser Facility, CLRC Rutherford-Appleton Laboratory, Chilton, Didcot, Oxfordshire OX11 0QX, UK

Erik T. J. Nibbering

Max-Born-Institut für Nichtlineare Optik und Kurzzeitspektroskopie, Rudower Chaussee 6, D-12489 Berlin, Germany

Paolo Foggi and Frederik V. R. Neuwahl

LENS, Largo E. Fermi 2, Florence, Italy

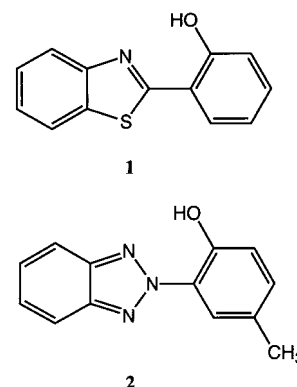
Received: August 29, 2000; In Final Form: January 3, 2001

Ultrafast pump–probe studies of room-temperature solutions of 3-hydroxyflavone (3-HF) and some 4'-substituted derivatives have been undertaken. Transient absorption attributable to the two zwitterionic forms of the excited tautomer arising from excited-state intramolecular proton transfer (ESIPT) was observed across most of the visible spectral region. For 3-HF in methylcyclohexane and acetonitrile, the ESIPT was found to be so rapid that it was only possible to assign a time constant of 35 fs to the process. In ethanol, however, a time constant of 60 fs was determined. The slower ESIPT in this solvent was attributed to the greater strength of the solute–solvent interactions. For the derivatives of 3-HF in all three solvents, the ESIPT step was also found to be instrument-limited. In addition to the femtosecond kinetics, there was also a picosecond component of the kinetics that is attributed to ESPT in molecules that are intermolecularly hydrogen bonded to the solvent.

## Introduction

The design and characterization of compounds which undergo excited-state intramolecular proton transfer (ESIPT) continues to engage the interest of scientists throughout the world. In a typical system such as 2-(2'-hydroxyphenyl)benzothiazole (**1**), excitation of the “normal” or “enol” species with a UV photon forms the Franck–Condon  $S_1$  excited state, which rapidly undergoes ESIPT to produce the excited tautomer species ( $S_1'$ , often referred to as the “keto” form). Following decay to the ground state by radiative or nonradiative processes, reverse proton transfer occurs to yield the original ground-state enol. However, despite the continued interest in such systems, it is noticeable that there are few new molecular systems in addition to those covered in our reviews,<sup>1,2</sup> which are now some 5 years old. In contrast, the advances in ultrafast laser technology in recent years are now giving us access to experimental measurements of actual ESIPT rates.

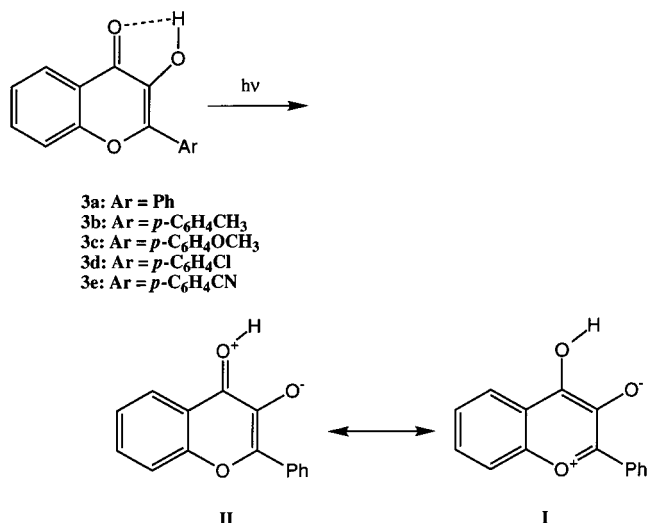
Of the studies of ESIPT rates that have been made, the majority involve compounds undergoing ESIPT to nitrogen, such as **1**, 2-(2'-hydroxy, 5'-methylphenyl)benzotriazole (Tinuvin-P, **2**), and [2,2'-bipyridyl]-3,3'-diol. Lärmer et al.<sup>3</sup> and Elsaesser et al.<sup>4</sup> have found a time constant of  $160 \pm 20$  fs for the ESIPT process for **1** in  $C_2Cl_4$ . Wiechmann et al.<sup>5</sup> and



Chudoba et al.<sup>6</sup> investigated the ultrafast dynamics of **2** in nonpolar solvents and attribute a rise component of about 100 fs to the proton-transfer reaction. A more recent paper by Chudoba et al.<sup>7</sup> claims to have detected vibrational coherence in the solvent response corrected, spectrally resolved transients observed from **2** with a time resolution of approximately 20 fs. Glasbeek's group have published a number of reports of their studies of the ultrafast emission properties of [2,2'-bipyridyl]-3,3'-diol.<sup>8–10</sup> In all cases, the ESIPT was too fast for them to measure and an upper limit of 300 fs was placed on the rise time. More recent work by Neuwahl et al. places an upper limit of <50 fs on this parameter.<sup>11</sup> Sekikawa et al.,<sup>12</sup> Kobayashi et al.,<sup>13</sup> and Mitra and Tamai<sup>14</sup> have reported measurement of

\* To whom correspondence should be addressed. Current address: School of Applied Sciences, University of Glamorgan, Pontypridd, Mid Glamorgan CF37 1DL, Wales. Tel: 01443 482280. E-mail: rgbrown@glam.ac.uk.

## SCHEME 1



proton-transfer rates in thermochromic salicylideneanilines. The proton-transfer times are on the order of 1.00 ps in the solid phase,<sup>12,13</sup> 210 fs in cyclohexane, and 380 fs in ethanol.<sup>14</sup>

Measurements of the rate of ES IPT to oxygen are limited, as far as we are aware, to methyl salicylate and related systems and 3-hydroxyflavone (**3**, 3-HF). Herek et al.<sup>15</sup> have undertaken a study of the ultrafast dynamics of the methyl salicylate system in the gas phase using a femtosecond fluorescence depletion technique. Both short- and long-lived (up to 120 ps) transients were obtained, and a rise component of  $60 \pm 10$  fs was reported for the rate of proton transfer along the hydrogen bond. The excited-state dynamics of 3-hydroxyflavone has received significant interest in the literature. The anomalous fluorescence behavior of 3-HF was first reported in detail by Sengupta and Kasha.<sup>16</sup> It was proposed that the two emission bands that were observed corresponded to fluorescence from the Franck–Condon excited-state  $S_1$  (emission around 400 nm) and the tautomer  $S_1'$  produced by ES IPT (emission around 500 nm), as shown in Scheme 1. Following the initial report, the photophysics of **3** has been studied by a number of research groups.<sup>17–23</sup> Most attempts to measure ES IPT in noninteracting solvents have proved to be instrument-limited, although Ernsting and Dick<sup>23</sup> were able to calculate the ES IPT rate constant as  $7.4 \times 10^{11} \text{ s}^{-1}$  on the basis of line shapes in the jet-cooled emission of 3-HF.

Transient absorption measurements for 3-HF on an ultrafast time scale have been reported by several groups. Dzugan et al.<sup>24</sup> and Rullière and Déclémy<sup>25</sup> studied the transient spectra obtained after picosecond (approximately 30 ps fwhm) excitation of 3-HF in room-temperature solution and at reduced temperature, respectively. Both reports indicate that there is transient absorption over a wide wavelength range (400–750 nm) together with gain in the region of 500–600 nm due to tautomer emission. More recent work by Schwartz et al.<sup>26</sup> reported the first observation of the ES IPT process on an ultrafast time scale. Measurements of the transient absorption were undertaken for absorption at 620 nm after excitation with a 310 nm, 125 fs pump pulse. Biexponential kinetics was observed in all solvents, with subpicosecond and picosecond components being present. The fast transient absorption changes of 3-HF in dry methylcyclohexane (MCH) showed a resolved subpicosecond component of 210 fs convoluted with the 125 fs time integrated Gaussian instrumental function. In methanol, the ultrafast rise component was shown to fit to the instrument function convoluted with an 80 fs exponential rise component. Discussion

of the effect of hydrogen-bonding impurities leads the authors to suggest that a different mechanism is responsible for ES IPT in polar solvents. They suggest that the formation of hydrogen-bonded complexes creates *intermolecular* motions, which may play an important role in the tautomerization process.

Mühlpfordt et al.<sup>27</sup> measured transient absorption spectra for 3-HF on the femtosecond time scale and were able to confirm the general observations about the spectral range of the absorption shown in the picosecond work<sup>24,25</sup> and the biexponential kinetics observed by Schwartz et al.<sup>26</sup> However, they consider that the picosecond component of the kinetics derives from vibrational redistribution and (solvent) relaxation processes. Ormson et al.<sup>28</sup> report the excited-state transient spectra for 3-HF in methylcyclohexane with a resolution of  $\sim 200$  fs after excitation at 295 nm. Two distinct absorption bands are present, centered around 460 (blue) and 575 nm (green). Evolution of both of these bands is clearly resolved, showing the blue band shifting from approximately 430 to 460 nm in a few picoseconds. After this point the transient absorption spectrum remains approximately constant and simply decays with a lifetime on the order of 5 ns (the lifetime of the tautomer species). The shape of the green band also changes in time, but the evolution is somewhat contaminated by the laser fundamental at  $\sim 590$  nm.

In light of these transient spectra, we have undertaken ultrafast kinetic measurements to both aid our interpretation of the transient spectral data and to (hopefully) yield values for the ES IPT rate constant to compare with the work of Schwartz et al.<sup>26</sup> and Mühlpfordt et al.<sup>27</sup> The results of these measurements are reported here.

## Experimental Section

3-Hydroxyflavone was obtained from Aldrich Ltd. and was recrystallized from ethanol before use. The substituted 3-hydroxyflavones were prepared by the Algar–Flynn–Oyamada reaction<sup>29</sup> from 2-hydroxyacetophenone and the appropriate substituted benzaldehyde. Following workup and recrystallization, all the compounds exhibited melting points and NMR data in accord with literature data. All solvents were spectrophoto-metric grade from Aldrich Ltd. and were used as received.

Absorption spectra were recorded on a Hewlett-Packard 8452A diode array spectrophotometer and fluorescence spectra on either Perkin-Elmer LS5 or SPEX Fluoromax spectrofluorimeters in fully corrected mode. Fluorescence quantum yields measurements were performed on optically dilute samples using quinine sulfate in 0.1 mol dm<sup>-3</sup> perchloric acid as the quantum yield standard ( $\phi_f = 0.55$ ).<sup>30</sup> Fluorescence decay profiles were measured using the single photon counting technique<sup>31,32</sup> with the synchrotron radiation source at Daresbury<sup>33</sup> as the excitation source. The decay profiles were analyzed by computer convolution, and the goodness of fit was evaluated on the basis of  $\chi$ -squared values and the distribution of the residuals.

Ultrafast kinetic spectroscopy was carried out using the pump–probe technique<sup>32</sup> using femtosecond laser systems at the CLRC Rutherford-Appleton Laboratory (RAL), Oxfordshire, United Kingdom, and the Max-Born Institute für Nichtlineare Optik und Kurzzeitspektroskopie (MBI), Berlin, Germany. Transient absorption spectra in the 350–700 nm spectral interval were recorded at the European Laboratory for Non-Linear Spectroscopy (LENS), Florence, Italy.

The laser system at RAL is based on a Ti:sapphire oscillator (Spectra Physics Tsunami) and a Ti:sapphire regenerative amplifier (Spectra Physics Spitfire) pumped with a Q-switched intracavity frequency doubled Nd:YLF laser (Spectra Physics

Merlin). The fundamental output is tunable from 770 to 840 nm, with pulse energies of approximately 1 mJ at 1 kHz. Transient absorption measurements may be undertaken at a variety of wavelengths with pump tunability from a custom-designed optical parametric amplifier<sup>34</sup> and other nonlinear frequency mixing techniques. This technology offers two synchronized and widely tuneable (200–2200 nm) ultrashort pulses. The probe wavelength is selected by a 10-nm band-pass filter from a continuum generated in a 1-cm flowing water cell. The continuum produced was high power but multifilament, which ultimately limited the resolution of the system to  $\sim 230$  fs. Other mechanisms may also contribute, e.g., imperfect imaging. Signal processing is carried out by dividing signal and reference photodiode outputs in an analogue circuit to reduce pulse-to-pulse jitter and then measurement using a digital lock-in amplifier (EG&G 7206). The lock-in frequency of around 200 Hz is derived from a chopper in the pump arm, which superimposes a modulation only on the signal diode. The detection limit of the system is on the order of  $10^{-4}$  of absorption. Solutions of concentration 1 mM were employed in these measurements in a 1-mm path length cell with an excitation wavelength of 350 nm. The relative polarizations of the pump and probe beams were maintained at the magic angle.

The MBI system is based on a custom-built chirped mirror dispersion compensated Ti:sapphire laser oscillator capable of generating 10-fs laser pulses.<sup>35</sup> Amplification is initially in a regenerative cavity (after appropriate pulse stretching) and subsequently in a multipass amplifier to bring the output to approximately 1.5 mJ after recompression. The output is continuously monitored by a single shot second-harmonic FROG (frequency-resolved optical gating) instrument to give simultaneous measurement of pulse width and spectrum (and thereby, phase). The pulses produced in this manner are typically below 50 fs, 1 kHz and with a spectral extent centered around 800 nm. Transient absorption measurements were performed in a manner similar to those previously reported.<sup>36</sup> Pump and probe pulses are derived from frequency-doubling components of the spectrum created in a hollow fiber<sup>37</sup> by angle tuning a pair of BBO crystals to provide the desired wavelengths (this restricts the bandwidth of the pulses to the acceptance angle of the crystal). Following generation, the two beams are independently compressed in double-pass prism pairs and then directed to the sample using all reflective optics. The sample is flowed through a dye laser jet to produce a path length of approximately 100  $\mu\text{m}$ . Solutions of 6 mmol concentration were used to give significant absorption at the pump wavelength of 360 nm. Changes in the probe transmission were monitored using a silicon photodiode and read to a computer via a time-gated analogue-to-digital converter at the laser repetition rate. The probe was referenced to a second photodiode measuring probe intensity prior to the sample jet. Changes in transmission of  $10^{-4}$  are achievable, providing many experiments are averaged to provide good statistics. The resolution of the system is on the order of 50–80 fs, as determined by cross-correlation in BBO or the sample jet.

The LENS system comprises a master oscillator (Spectra Physics Tsunami Ti:sapphire laser) pumped by an intracavity frequency doubled cw Nd:YVO laser (Spectra Physics Millennium). The short ( $< 70$  fs) pulses from the oscillator are stretched and amplified at 1 kHz repetition rate by a regenerative amplifier (BMI Alpha 1000). After compression, a total average power of 750–800 mW and pulse duration of 90–100 fs are obtained. The tunability of the pulses in the UV–visible range is achieved by pumping an optical parametric generator and amplifier

(OPG–OPA) based on a BBO crystal (prototype of TOPAS by Light Conversion, Vilnius, Lithuania).<sup>38,39</sup> About 700 mW of the output is utilized to pump the OPG–OPA, and tunable pulses are obtained in the 2.4–1.2- $\mu\text{m}$  wavelength interval, with a conversion efficiency on the order of 35%. Two 0.3 mm thick BBO crystals placed at the outlet of the OPG–OPA are utilized to carry out the wave-mixing processes needed for the pulse to cover the whole of the spectral range from 240 to 800 nm.<sup>39</sup> The pulse duration, determined by second-order autocorrelation using stimulated Raman gain directly in the sample, is always less than 90 fs in the range 500–800 nm. A broad band UV–visible continuum acts as the probe pulse. A small portion of the 800-nm radiation (1–2 mW) is utilized to generate a continuum light useable in the range from 250 nm in the UV up to 1.4  $\mu\text{m}$  in the NIR, although the optical setup is optimized for the 350–700 nm wavelength range. The continuum is obtained by focusing about 1 mW of the beam from the regenerative amplifier into a 2.5 mm thick calcium fluoride plate. The power density in the focus is carefully adjusted in order to operate in the single filament regime. In this way it is possible to obtain a stable and well-collimated beam of continuum radiation. The white light beam is split into two parts of equal intensity by a 50/50 quartz beam splitter. One-half (the probe pulse) is used to measure the transient spectrum by passing it through the excited sample at some known time after the excitation (pump) pulse. The other half of the continuum acts as a reference pulse, travelling through a shorter optical path and hence interacting with the sample prior to the excitation process. This setup provides a convenient normalization function for the transient spectrum, significantly increasing the signal-to-noise ratio. To prevent the lengthening of the instrumental function due to group velocity mismatch between pump and probe, a thin (0.3 mm) flowing cell is utilized for the sample. The white light continuum is temporally dispersed over almost 1 ps between 350 and 700 nm. To simplify the experimental setup, it is used like this without any correction. However this must be taken into account in the analysis of the spectral evolution in the first picosecond following excitation. Multi-channel detection is achieved by an AR coated, back-illuminated 1100  $\times$  330 CCD camera (Princeton Instruments TE/CCD-1100-BP/VISAR). The range of its spectral response is from 300 nm to 1  $\mu\text{m}$ , with a maximum quantum efficiency of 80% between 600 and 700 nm. Two horizontal strips were selected on the CCD target, corresponding to the spectrum of the probe and the reference dispersed by a 300 grooves/mm grating of a 25 cm flat field Czerny–Turner spectrograph (Chromex 250). All the measurements were undertaken with both the pulses linearly polarized and at the magic angle.

## Results

**Steady-State Absorption and Emission Properties.** Steady-state absorption and emission spectra were measured for 3-hydroxyflavone (**3a**), 4'-methyl-3-hydroxyflavone (**3b**), 4'-methoxy-3-hydroxyflavone (**3c**), 4'-chloro-3-hydroxyflavone (**3d**), and 4'-cyano-3-hydroxyflavone (**3e**) in methylcyclohexane, ethanol, and acetonitrile at ambient temperatures, together with their emission quantum yields. These data are shown in Table 1. It is immediately noticeable that the various substituents have only a small effect on the absorption and emission properties of 3-hydroxyflavone: a slight red shift in absorption and emission, but no major effect on the quantum yield.

**Transient Absorption Spectra.** Transient absorption spectra were measured for **3a–3e** in methylcyclohexane, ethanol, and acetonitrile at ambient temperatures using the LENS system.

**TABLE 1: Steady State Absorption and Emission Properties for 3a–3e in Methylcyclohexane (MCH), Acetonitrile, and Ethanol**

compd	solvent	$\lambda_{\max}^{\text{abs}}$ , nm (log $\epsilon_{\max}$ )	$\lambda_{\max}^{S_1}$ , nm	$\lambda_{\max}^{S_1'}$ , nm	$\phi_{\text{em}}$
3a	MCH	340 (4.27)	—	525	0.24
	ethanol	345 (4.19)	402	533	0.01
	acetonitrile	341 (4.34)	389	526	0.04
3b	MCH	342 (4.32)	—	528	0.32
	ethanol	348 (4.51)	407	535	0.03
	acetonitrile	344 (4.36)	387	528	0.07
3c	MCH	350 (4.29)	—	529	0.27
	ethanol	356 (4.40)	426	533	0.03
	acetonitrile	350 (4.47)	428	531	0.03
3d	MCH	342 (4.37)	—	531	0.25
	ethanol	347 (4.32)	407	535	0.02
	acetonitrile	344 (4.42)	400	529	0.05
3e	ethanol	350 (4.41)	412	543	0.03
	acetonitrile	346 (4.20)	402	533	0.06

Measurements were also undertaken on some 4'-amino derivatives of 3-hydroxyflavone, but these were found to be complicated by the intense fluorescence associated with TICT state formation,<sup>40</sup> and these data will be reported in a later paper.

Transient absorption spectra for **3a** have been previously reported by us.<sup>28</sup> Subsequent measurements show that the absorption observed around 575 nm<sup>28</sup> is actually part of a band that was obscured by the laser fundamental in our initial work. The transient spectra for **3a** and the spectra recorded for **3b–3e** are very similar. We therefore show spectra for **3d** in the three solvents (Figures 1–3) as being largely typical of the behavior of all five compounds in these solvents. In methylcyclohexane (Figure 1a), the initial transient absorption is in the region of 410 nm, but this intensifies and shifts to the red at longer delay times, until after approximately 1 ps, where a broad band is present that has its maximum around 470 nm with significant absorption across most of the wavelength range 400–550 nm. We call this first transient absorption the “blue band”.

After a few hundred femtoseconds, a second absorption band is also apparent in the red (the “red band”) with a maximum around 610 nm. Over the same time scale, a gain band, which lies between the two transient absorptions, also becomes apparent. On a longer time scale (Figure 1b), the blue band increases slightly in intensity, but the intensities of the red and the gain bands increase significantly. The relative intensities of these two latter bands appear to be correlated.

The transient behavior of **3d** in ethanol and acetonitrile (Figures 2 and 3) is quite similar to that observed in methylcyclohexane. Both blue and red transient absorption bands are present, although the red band is less pronounced at early time scales (Figures 2a and 3a) than in methylcyclohexane. A gain band, lying between the two transient absorption bands, is again observed. The kinetics of the transients from **3d** (and **3a–3c**) in these three solvents on qualitative analysis therefore appear to reproduce the kinetics of **3a** reported by Schwartz et al.<sup>26</sup> in that (at least) ultrafast (subpicosecond) and fast (picosecond) components are involved in the formation of all three bands.

4'-cyano-3-hydroxyflavone (**3e**) exhibits a significant variation on the general behavior observed for **3a–3d**. As Figure 4 shows, in ethanol and acetonitrile (**3e** is insufficiently soluble in methylcyclohexane for quality data to be recorded) the blue and red transient absorption bands are still in evidence, albeit the former is at slightly higher wavelength compared to **3a–3d**. A gain band is not observed, but the evolution of the shape of the transient absorption around 550 nm certainly evokes the gain bands seen in Figures 2a and 3a. However, the significant difference observed for **3e** is that the blue band decays over a

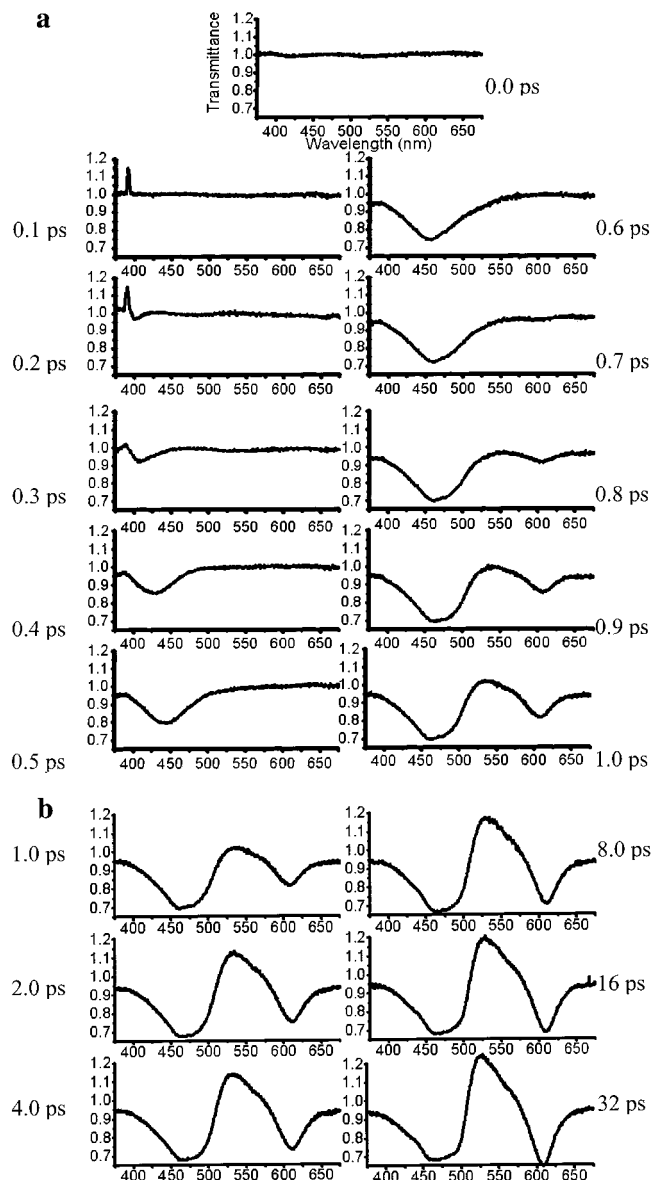


**Figure 1.** Transient spectra of **3d** in methylcyclohexane following excitation at 350 nm: (a) 0–1 ps delay and (b) 1–32 ps delay.

time scale of 1–100 ps with a concomitant rise in the red band. This behavior is unique to compound **3e**.

**Transient Kinetics. 3a in Methylcyclohexane.** The transient absorption of 3-hydroxyflavone in methylcyclohexane was monitored at a range of wavelengths across the transient absorption bands using the RAL system. These wavelengths were chosen in the light of our previous suggestion that transient absorption around 430 nm could be attributed to the  $S_1$  state (excited enol) and absorption above 450 nm to the  $S_1'$  state (excited keto). Transient kinetics was therefore recorded at 420, 450, and 480 nm, together with 585 and 620 nm, to both provide data for comparison with the earlier work of Schwartz et al.<sup>26</sup> and to probe the red transient band.

At all wavelengths, a rapid rise in the transient absorption was observed (Figure 5), together with a further small rise at longer times at the longer monitoring wavelengths of 585 and 620 nm. There was some evidence of a longer lived component in the transient absorption between 420 and 480 nm, but its intensity was very low. The kinetic profiles were all fitted to one or a sum of two or three exponential rise components (lifetime  $\tau_i$  and pre-exponential factor  $A_i$ ) convoluted with a Gaussian instrumental response. In all cases the fast rise was

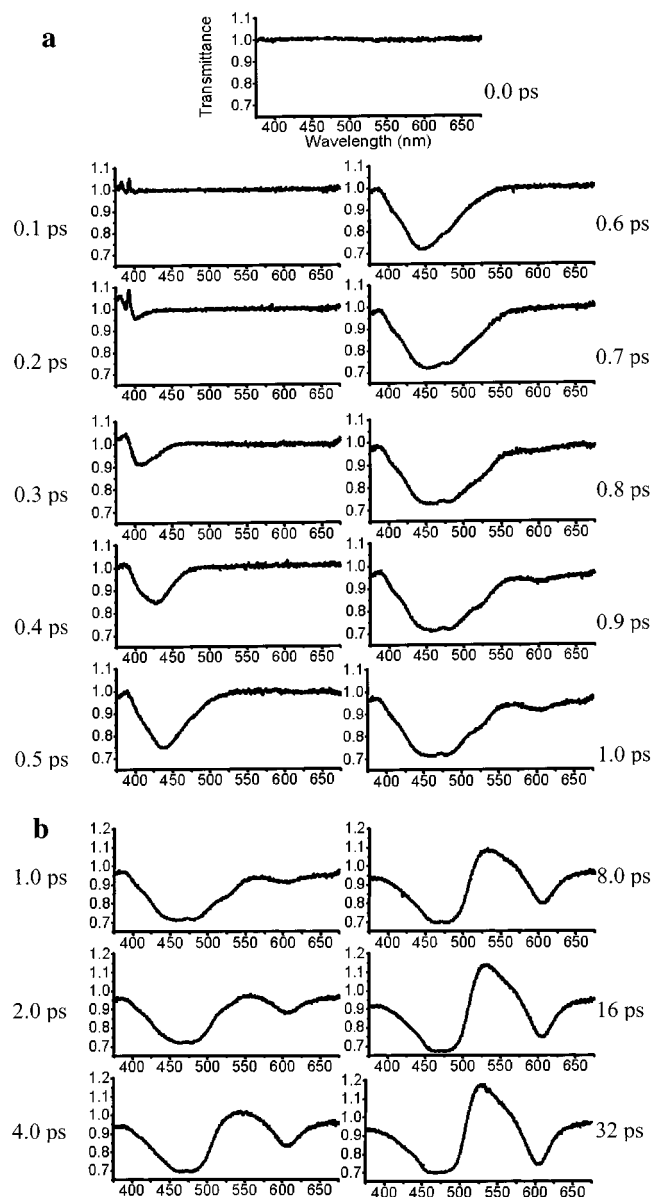


**Figure 2.** Transient spectra of **3d** in acetonitrile following excitation at 350 nm: (a) 0–1 ps delay and (b) 1–32 ps delay.

found to be beyond the time resolution of the RAL system. In light of these results, we feel that the best that can be achieved is an upper limit on the fast rise time of 100 fs. We consider this value to be the limit of the deconvolution that is possible given the pulse width of the RAL system and the quality of the data. The rise time of the longer lived component is calculated as 10 ps at a probe wavelength of 585 nm and 1.6 ps at 620 nm. The intensity of this component of the transient absorption is low compared to the intensity of the fast-rise component, and this is reflected in the disparity in the two values for the rise time reported above. We also report the ratio of the two pre-exponential (intensity) factors  $A_1/A_2$  in Table 2.

The transient kinetics of 3-HF in methylcyclohexane was remeasured at MBI. Here we are restricted in the choice of probe wavelengths, although the time resolution is better. We therefore only measured kinetic traces at a probe wavelength of 440 nm. The kinetic traces were fitted to either a single rise component or, as in the case of the example data shown in Figure 6, to a sum of two components. In the case of Figure 6, the second component is a decay with a 1.0 ps lifetime. However, the value of 1.0 ps is not well-characterized by the MBI experiments, as

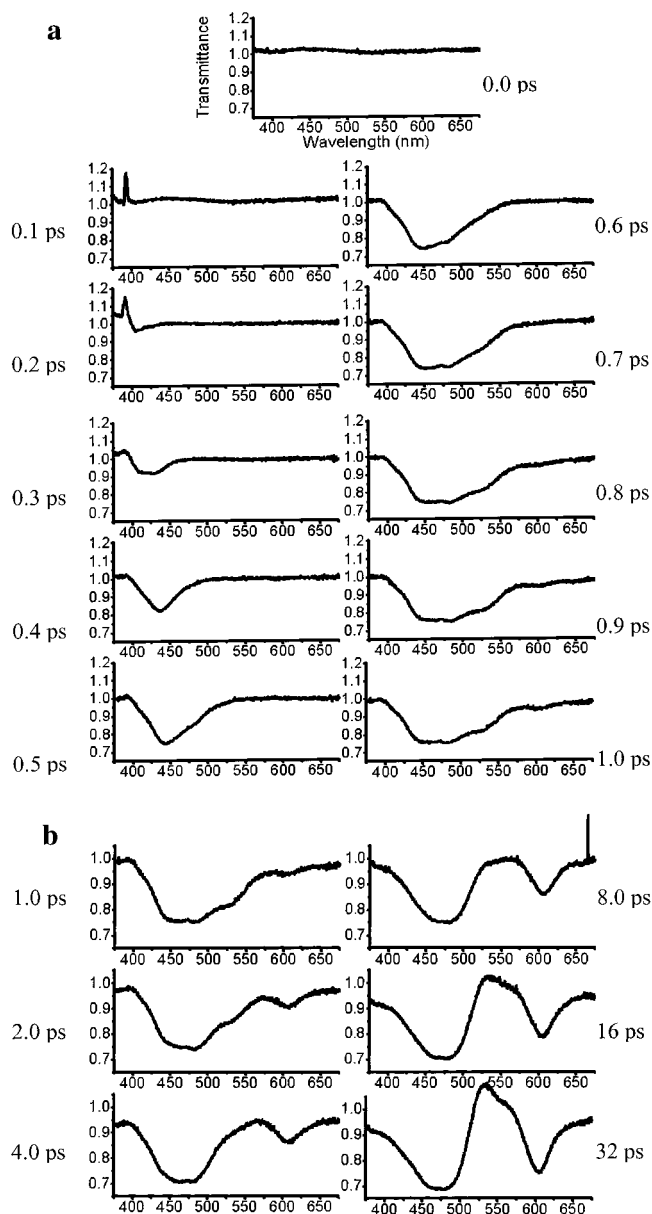


**Figure 3.** Transient spectra of **3d** in ethanol following excitation at 350 nm: (a) 0–1 ps delay and (b) 1–32 ps delay.

the time-scale is too short. The use of two components usually gave slightly better fits, but the marginal improvement in the quality of the fit together with the scatter of the data leads us to question whether the 1.0 ps component is real. There is certainly no evidence for this component in the RAL data of Figure 5. As regards the fast-rise component, we once again find that it is instrument-limited, such that an upper limit of 35 fs is all that we can assign to it, using identical reasoning to that above.

All the results are collated in Table 2.

**3a in Acetonitrile.** The transient absorption spectra observed for 3-HF in acetonitrile are very similar to those observed for methylcyclohexane as solvent. The same set of probe wavelengths was therefore chosen for parallel experiments to those for 3-HF in methylcyclohexane at both RAL and MBI, with very similar outcomes, namely, that two rise components are observed. Again, the fast component is unresolved at both RAL and MBI, and the same upper limits as proposed for the methylcyclohexane experiments are suggested here (Table 2). The slow component is well-resolved in the RAL data and has a rise time of 5 ps at all wavelengths.

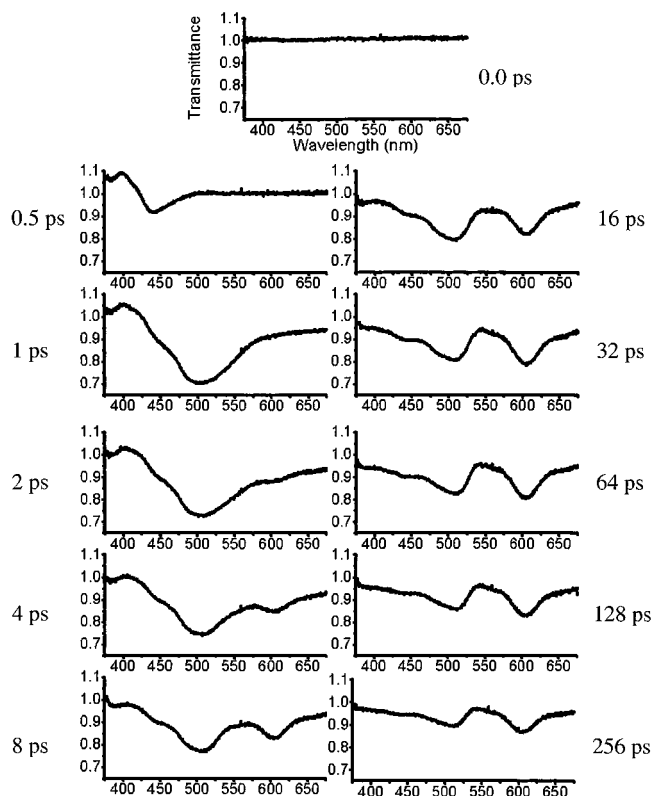


**Figure 4.** Transient spectra of **3e** in ethanol following excitation at 350 nm with delays of 0–256 ps.

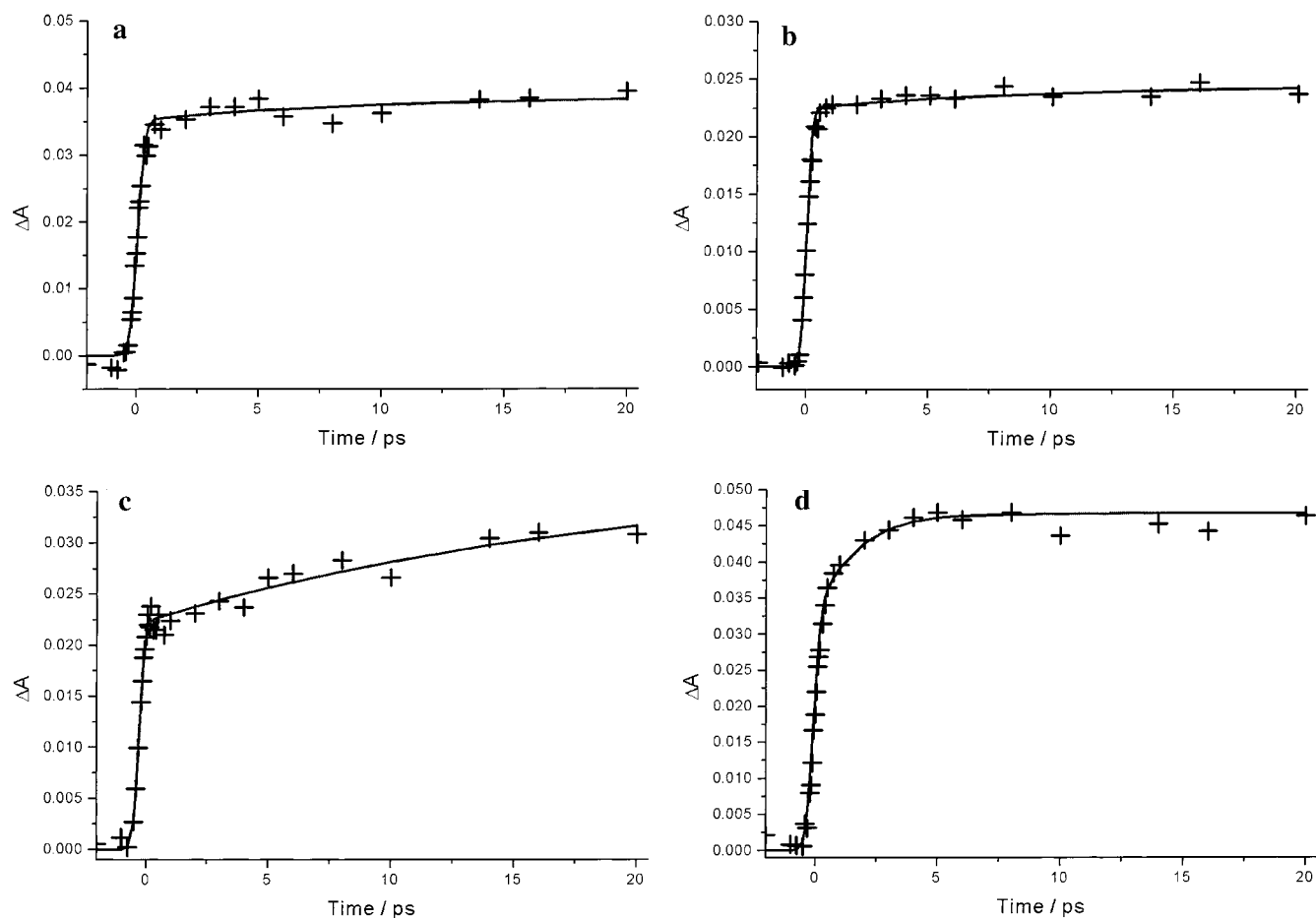


**Figure 5.** Transient kinetics of 3-hydroxyflavone (**3a**) in methycyclohexane probed at (a) 450 nm, (b) 480 nm, (c) 585 nm, and (d) 620 nm following excitation at 350 nm with the RAL system. The rise times for the fitted curves are given in Table 2.

**3a in Ethanol.** Identical comments may be made regarding the transient absorption spectra of 3-HF in ethanol, and the same series of probe wavelengths have again been employed here. The observed kinetics at all wavelengths in the RAL experiments are bicomponent (Figure 7a) with rise times of 10 ps (slower component) and an instrument-limited response for the fast rise. The MBI data appears to allow the fast rise to be resolved, and a value of 60 fs together with a 1.0 ps decay component gives the best fit to the experimental data (Table 2 and Figure 7b). The fast rise in ethanol is compared with that observed in methylcyclohexane in Figure 8. The data of Figure 7b gives more confidence that the 1.0-ps component is real, but once again, it is absent from the RAL data (Figure 7a). The major difference between the RAL and MBI experiments is a 6-fold increase in concentration for the latter. We therefore conclude that the 1.0-ps decay in the MBI data relates to a self-quenching process. However, this assignment is still tentative, and we have not ruled out solvent relaxation processes, even though this component is apparently absent from the RAL data.

**3b–3e in Methylcyclohexane, Ethanol, and Acetonitrile.** The kinetics of the transients observed for **3b–3e** in the three solvent systems was only studied at LENS. Kinetic traces were reconstructed from the transient spectra as a function of time by averaging the data for a 10-nm bandwidth around the wavelength of interest and plotting the transient absorbance as a function of the time delay. Kinetic analysis of multiple wavelengths in each of the three transients rapidly established that there was very little difference with wavelength across the blue and red absorption bands and the gain band. We therefore

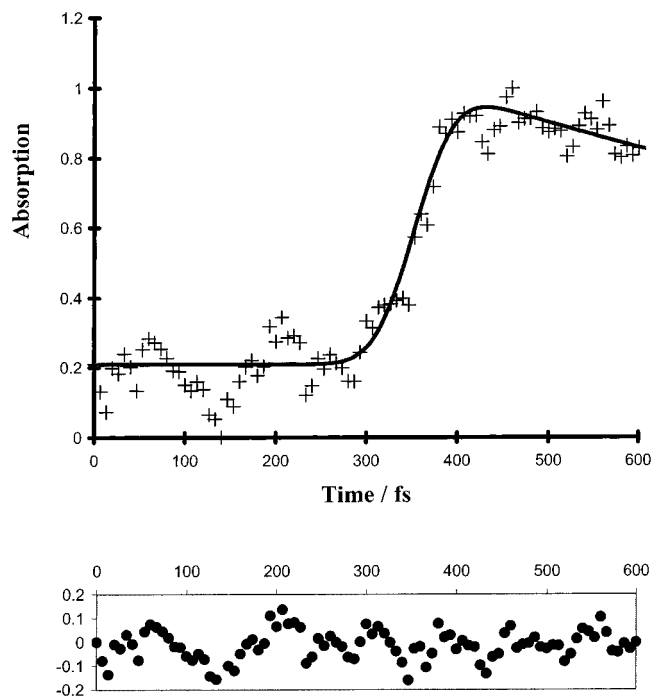


**Figure 6.** Transient kinetics and residuals for 3-hydroxyflavone (**3a**) in methycyclohexane probed at 440 nm following excitation at 360 nm with the MBI system. The rise times for the fitted curve are given in Table 2.

**TABLE 2: Transient Kinetics Observed for Room Temperature Solutions of 3-Hydroxyflavone at Various Probe Wavelengths**

solvent	probe wavelength, nm	$\tau_1$ , fs	$\tau_2$ , ps	$A_1/A_2$	system
MCH	420	100	$10.0 \pm 0.5$	14.2	RAL
	440	35	—	—	MBI
	450	100	$10.0 \pm 0.5$	16.4	RAL
	480	100	$10.0 \pm 0.5$	12.1	RAL
	585	100	$10.0 \pm 0.5$	2.2	RAL
acetonitrile	620	100	$1.6 \pm 0.5$	2.1	RAL
	420	100	$5.0 \pm 0.5$	3.3	RAL
	440	35	—	—	MBI
	450	100	$5.0 \pm 0.5$	1.2	RAL
	480	100	$5.0 \pm 0.5$	2.2	RAL
ethanol	585	100	$5.0 \pm 0.5$	0.6	RAL
	420	100	$10.6 \pm 0.5$	1.0	RAL
	440	$60 \pm 20$	—	—	MBI
	450	100	$10.0 \pm 0.5$	1.8	RAL
	480	100	$10.0 \pm 0.5$	2.8	RAL
	585	100	$10.0 \pm 0.5$	0.6	RAL

report the results for a single wavelength in each of the transient bands for each compound in each solvent.

The kinetic data were once again fitted to a sum of exponential rise components, and kinetic traces similar to those shown in Figure 5 were obtained. All samples exhibited an instrument-limited initial rise identical to that for **3a**. In addition, either one or two picosecond components were also observed in the kinetics (Table 3). In the cases of the blue and red transients, the picosecond components have positive pre-exponential factors ( $A_2$  and  $A_3$ ), indicative of a further increase of transient absorption. The corresponding pre-exponential factors for the gain band are negative, indicating increased emission on a picosecond time scale (Table 3). The one exception to these general observations is, unsurprisingly, **3e**, where the transient spectra (Figure 4) indicate decay of the blue

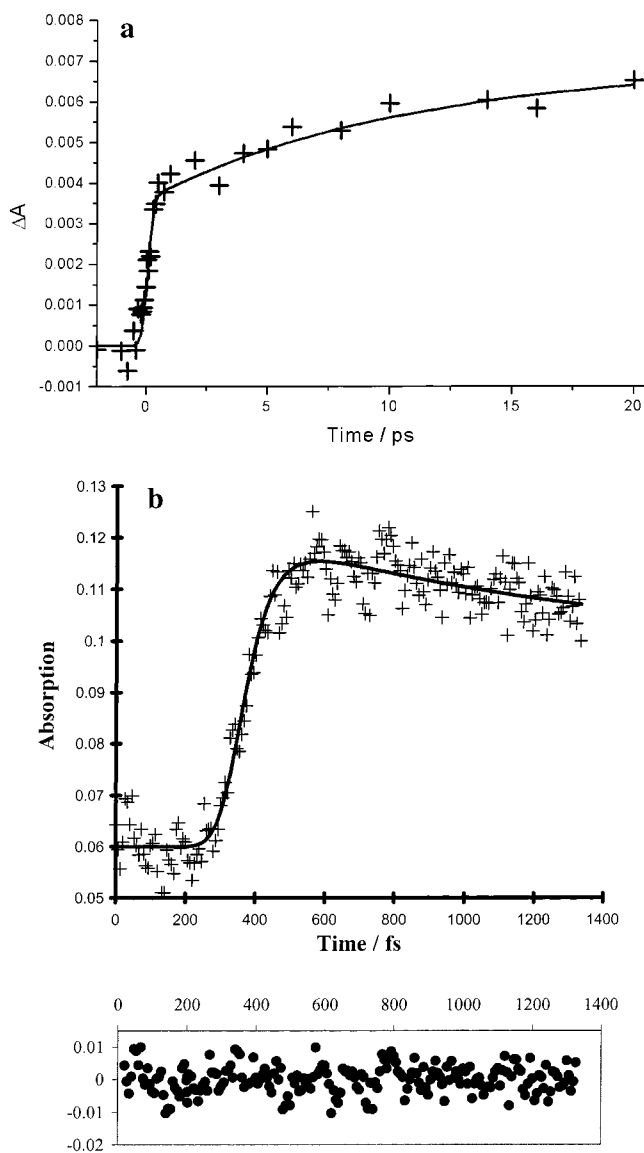


**Figure 7.** Transient kinetics and residuals (for the MBI data) of 3-hydroxyflavone (**3a**) in ethanol probed at (a) 420 nm following excitation at 350 nm with the RAL system and (b) 440 nm following excitation at 360 nm with the MBI system. The rise times for the fitted curves are given in Table 2.

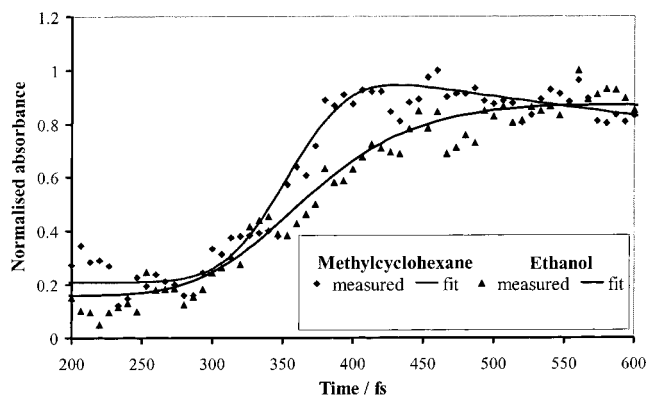


**Figure 8.** Direct comparison of transients from 3-hydroxyflavone (**3a**) in methycyclohexane and ethanol (pump 360 nm, probe 440 nm).

transient (negative  $A_2$ ) with a concomitant increase in the red transient. The fitted lifetimes and pre-exponential factors are all collated in Table 3.

**TABLE 3: Transient Kinetics Observed for Room Temperature Solutions of Substituted 3-Hydroxyflavones 3b–3e at Various Probe Wavelengths**

compd	$\lambda$ , nm	methylcyclohexane			ethanol			acetonitrile		
		$\tau_1$ , fs ( $A_1$ )	$\tau_2$ , ps ( $A_2$ )	$\tau_3$ , ps ( $A_3$ )	$\tau_1$ , fs ( $A_1$ )	$\tau_2$ , ps ( $A_2$ )	$\tau_3$ , ps ( $A_3$ )	$\tau_1$ , fs ( $A_1$ )	$\tau_2$ , ps ( $A_2$ )	$\tau_3$ , ps ( $A_3$ )
3b	460	<200 (0.79)	1.5 (0.21)	—	<200 (0.33)	11.0 (0.67)	—	<200 (0.55)	5.0 (0.45)	—
	530	<200 (0.44)	1.5 (−0.17)	9.5 (−0.49)	<200 (0.43)	11.0 (−0.57)	—	<200 (0.28)	4.0 (−0.72)	—
	600	<200 (0.67)	9.5 (0.33)	—	<200 (0.76)	11.0(0.24)	—	<200 (0.31)	5.0 (0.69)	—
3c	460	<200 (1.00)	—	—	<200 (1.00)	—	—	<200 (0.31)	5.5 (0.31)	—
	530	<200 (−0.77)	3.0 (0.23)	—	<200 (0.39)	9.0 (−0.61)	—	<200 (0.30)	5.5 (−0.70)	—
	600	<200 (1.00)	—	—	<200 (0.43)	1.5 (0.57)	—	<200 (0.30)	5.5 (0.70)	—
3d	460	<200 (0.86)	12.0 (0.14)	—	<200 (0.88)	12.0 (0.12)	—	<200 (0.78)	6.0 (0.22)	—
	530	<200 (0.31)	0.5 (−0.51)	12.0 (−0.18)	<200 (0.46)	11.0 (−0.54)	—	<200 (0.36)	0.4 (−0.12)	6.0 (−0.52)
	600	<200 (0.63)	12.0 (0.37)	—	<200 (0.33)	12.0 (0.67)	—	<200 (0.33)	6.0 (0.67)	—
3e	460	—	—	—	<200 (0.75)	1.4 (−0.19)	27.0 (−0.06)	<200 (0.71)	8.2 (−0.29)	—
	500	—	—	—	<200 (0.66)	1.9 (−0.13)	27.0 (−0.21)	<200 (0.73)	8.5 (−0.27)	—
	530	—	—	—	<200 (0.55)	5.0 (−0.24)	27.0 (−0.21)	<200 (0.63)	7.0 (−0.37)	—
	600	—	—	—	<200 (0.51)	5.1 (0.49)	—	<200 (0.39)	1.2 (0.44)	7.0 (0.17)

## Discussion

**The Origin of the Blue and Red Transients.** Transient absorption spectra on a fast time scale for 3-hydroxyflavone have been reported by four research groups. Dzugas et al.<sup>24</sup> and Rullière and Déclémy<sup>25</sup> undertook measurements using picosecond pulse excitation, and subpicosecond measurements have been undertaken by Mühlfordt et al.<sup>27</sup> and ourselves.<sup>28</sup> In all cases it is clear that transient absorption occurs across the whole of the visible spectral range with peaks in the region of 450 (blue band) and 610 nm (red band), as seen in Figures 1–4. The transient spectra in the region of between (approximately) 500 and 600 nm are complicated by stimulated emission from the 3-HF tautomer excited state.

The spectral shapes of the transient bands measured by Dzugas et al. and our group are largely independent of the time delay between excitation and measurement of the transient spectrum (taking into account the experimental reproducibility). The same is largely true for the low-temperature data of Rullière and Déclémy, although they report two distinct transient emission bands. Mühlfordt et al. also consider that there is some change in the shape of the gain band as a function of time, but one has to be cautious in assigning significance to these observations, given that the gain band is comprised of contributions from transient absorption and stimulated emission.

However, it is very noticeable in our results and elsewhere<sup>24,25,27</sup> that the relative intensities of the two bands change with time. For example, in the work of Mühlfordt et al.,<sup>27</sup> the blue band is about twice as intense as the red band at the earliest measured time (153 fs delay), whereas it is the latter that is more intense at longer times (approximately 7 ps). This behavior is also noticeable in the kinetic traces that we have measured. In virtually all cases the rise of the transient absorption is biexponential with an ultrafast (virtually always instrument-limited) component and a slower, picosecond component. In MCH the latter is only present in the kinetic traces for the blue transient absorption at very low intensity. In the other two solvents, the relative amount of the picosecond rise component is always much greater for the red band, as evidenced by the ratio of the intensity factors  $A_1/A_2$  in Tables 2 and 3.

We have already noted that 4'-cyano-3-hydroxyflavone (**3e**) exhibits transient absorption kinetics that is significantly different than those of the other four compounds (Figure 4). The blue and red transient absorption bands are both in evidence, but on a picosecond time scale, the blue band decays into the red band. Dzugas et al.<sup>24</sup> and Schwartz et al.<sup>26</sup> consider that both the blue and red transient absorption bands are derived from the same excited electronic state of the tautomer. The latter observe essentially identical kinetics for **3a** in methylcyclohexane at 540

and 620 nm. This contrasts with the results presented here and those of Mühlfordt et al., where the relative amounts of the ultrafast and picosecond components vary with wavelength. Additionally, Rullière and Déclémy considered that they observed the excited normal form as part of the blue transient absorption, a conclusion that we also drew in our preliminary work.<sup>28</sup>

We have to conclude that in all the transient absorption data (both femtosecond and picosecond) that have been reported for 3-HF, there are contributions from at least two absorbing species. The evidence for this is the wavelength-dependent multiexponential kinetics observed for **3a–3e**, especially the apparent parent–daughter relationship between the blue and red bands for **3e**. We have not observed this relationship for any of the other compounds, which may reflect the fact that the increase in absorption due to the picosecond component either balances (methylcyclohexane) or outweighs (ethanol and acetonitrile) any decrease. Alternatively, the picosecond rise component may have its origin in a species that is “hidden”, i.e., that does not absorb in the visible at the wavelengths that we and others have probed.

If we consider the species which could give rise to the observed transient absorption, there are three possible candidates, namely, the excited normal form ( $S_1$ ), an excited tautomer ( $S_1'$  or  $T_1'$ ), or the tautomer ground state ( $S_0'$ ). Although the transient spectra reported here and those in our preliminary report<sup>28</sup> suggest that there may be absorption in the region of 420 nm at the earliest delay times that could be attributed to  $S_1$ , our data exhibits no discernible difference in the ultrafast rise time for a given solvent with probe wavelength, except for changes in the overall intensity. In particular, at 420 nm there is no evidence for either a rapid rise followed by a rapid decay or a bicomponent rapid rise, which would be expected on the basis of our previous suggestion that the  $S_1$  state absorbs around 420–430 nm.<sup>28</sup> However, given that we have been unable to resolve a rise time for the formation of the transient absorption bands, it is entirely probable that the rise and decay of  $S_1$  are so rapid that they simply convolute in with the rise of the blue and red transient absorptions. Although Rullière and Déclémy also considered that the normal form contributed to their blue transient absorption, no one else has reported experimental data to corroborate this, and therefore, we conclude that this assignment has to be treated with caution. However, we believe that the lifetime of the excited enol is very short and that it is reasonable to conclude that, after a few hundred femtoseconds, neither the blue nor the red transient derive from  $S_1$ .

It is also possible to eliminate the ground-state tautomer  $S_0'$  from consideration. Although the reported spectrum of  $S_0'$  overlaps significantly with that of our blue transient,<sup>41</sup> the



spectrum of  $S_0'$  differs significantly from that of the blue transient. Indeed, in the nanosecond data of Itoh and Fujiwara,<sup>41</sup> the earliest spectra, which look very similar to our blue transient, are observed to decay into the spectrum assigned to  $S_0'$ . In addition, the lifetime of the excited tautomer of approximately 4 ns<sup>28</sup> indicates that  $S_0'$  will not be formed in substantial quantities on the time scale of our experiments.

The two species that appear to be present therefore derive from the excited tautomer following ESPT. Both species are formed on both ultrafast (subpicosecond) and fast (picosecond) time scales, and we see no reason to disagree with the assignment of Schwartz et al. that the two time scales relate to molecules which are intramolecularly (fs time scale) and intermolecularly (with the solvent and on a ps time scale) hydrogen-bonded at the time that they are photoexcited (i.e., molecules that undergo ESIPT and either solvent-assisted proton transfer or desolvation followed by ESIPT, respectively). The two transient absorptions have been found to display similar decay times that are effectively identical to the decay time of the tautomer emission.<sup>26,28</sup> We conclude from this that the excited triplet tautomer does not contribute substantially to the observed transients that must therefore both derive from the first excited singlet state of the tautomer  $S_1'$ . We therefore propose that the blue and red transient absorption bands correspond to the tautomeric forms I and II respectively in Scheme 1.

In addition to the reasoning outlined above, we consider that the red transient is II because this proton-transfer product may be stabilized by hydrogen bonding to the solvent molecules that have either participated in or slowed the picosecond proton-transfer reaction. We also consider that the 4'-cyano substituent will destabilize I with respect to II because a positive charge at the 2-position of the pyran ring will be disfavored by an electron-withdrawing substituent in the 2-phenyl ring. This would explain the redistribution of absorption intensity observed in Figure 4. However, there is no obvious evidence that the converse is true, i.e., that electron-donating groups stabilize I with respect to II.

**The Speed of ESIPT in 3a–3e.** Our results clearly suggest that ESIPT in room-temperature solutions of 3-HF is more rapid than indicated by the previous measurements of Schwartz et al.<sup>26</sup> and Mühlfordt et al.<sup>27</sup> The RAL system employed here for the majority of the measurements is similar to the equipment used by Schwartz et al. in terms of the time resolution, although we have access to a greater range of wavelengths to probe the transient kinetics. However, at all probe wavelengths we can only assign a maximum value to the ESIPT rise time of 100 fs from the RAL data and 35 fs (in MCH and acetonitrile) from the MBI data. We therefore conclude that the measurements of Schwartz et al. (and probably Mühlfordt et al.) are also instrument-limited and that the values reported by them represent lower limits for the ESIPT rate. It is known that small amounts of hydrogen-bonding impurities such as water influence the emission properties<sup>20</sup> and transient kinetics<sup>26</sup> of 3-HF, but we feel that this is unlikely to be the cause of the discrepancy between the results reported here and those of previous workers,<sup>26,27</sup> given that the only ultrafast rise time that we have found that is not instrument-limited is that for 3-HF in the hydrogen-bonding solvent ethanol.

The only ultrafast rise time that we have been able to definitely assign a value to here is that in ethanol (60 fs). The ESIPT rate in MCH and acetonitrile is more rapid. Figure 8 shows that the rise time in ethanol is definitely longer than in methylcyclohexane, thus validating our ability to assign a rise time in ethanol. We would expect that the interaction between

the solute 3-HF and the solvent would be strongest in ethanol, and this is evidenced by the (slightly) slower rise time for the tautomer transient absorption in this solvent. The 3-HF is assumed to be involved in both intra- and intermolecular hydrogen bonding, with the latter (involving one or more ethanol molecules) weakening the intramolecular hydrogen bond and thus decreasing the ESIPT rate. This conclusion is the reverse of that drawn by Schwartz et al.,<sup>26</sup> who attributed the increased ESIPT rate in methanol to the formation of a 3-HF monosolvate complex. However, our 60 fs rise time in ethanol is very similar to the 80 fs they report in methanol.

We can compare the ESIPT rates measured here with those reported by Herek et al.<sup>15</sup> for methyl salicylate, albeit the latter were measured in the gas phase with no interference from a solvent. Herek et al. report a rise time of  $60 \pm 10$  fs for ESIPT, which is identical to the value we find for 3-HF in ethanol. Their experimental value was rather longer than the 13 fs predicted on the basis of the O–H stretching frequency in methyl salicylate, and this was attributed to dispersion of the wave packet in the excited state due to torsional motions and intramolecular vibrational energy redistribution (IVR). The magnitude of the proton-transfer time in Tinuvin-P (**2**) is also attributed to a low-frequency vibrational mode at  $469 \text{ cm}^{-1}$ , which modulates the two subunits of the molecule with respect to one another, opening up a channel for proton transfer along the hydrogen-bond coordinate.<sup>7,42</sup> The 3-HF has less steric freedom than methyl salicylate and Tinuvin-P, so torsional motions affecting the intramolecular hydrogen bond may have less effect on the excited-state wave packet. The ESIPT rate for 3-HF in MCH and acetonitrile may therefore be quite close to the 10–20 fs expected on the basis of the O–H stretching frequency. As previously noted, the slower ESIPT rate for 3-HF in ethanol can be rationalized in terms of stronger excited state–solvent interactions, although IVR may well play a part here as well.

Finally, we consider the origin of the slower, picosecond rise component that is observed in most of the experiments reported here. The rise time for this component is solvent dependent (Tables 2 and 3) and the relative intensity of this component compared to the ultrafast ESIPT component depends on the probe wavelength. The first of these observations would certainly be in accord with previous experimental results, which indicate the presence of intermolecular hydrogen-bonded complexes in polar and protic solvents.<sup>26</sup> The picosecond rise time therefore presumably reflects the time required for the intermolecular hydrogen bond to be broken prior to the (rapid) proton-transfer process. Once again, the observation that this process is slower in ethanol than in acetonitrile can be reconciled in terms of the strength of the intermolecular solute–solvent interactions. However, it is also noteworthy that the rise times derived from the data are of a similar time scale to solvent relaxation, and the observed spectral changes could reflect these processes rather than a proton transfer reaction. However, it is also noticeable that the bands observed on the picosecond time scale (Figures 1b–3b and 4) do not exhibit any significant spectral shift, as might be expected as the result of solvent relaxation, only changes in overall intensity. We therefore conclude that the picosecond kinetic component does not result from solvent relaxation.

However, if the ESIPT process which follows the breaking of the intermolecular hydrogen bond with the solvent yields the same species as the immediate, ultrafast ESIPT, one would expect to see the same relative proportions of the two rise components across the whole of the transient absorption

spectrum. This is clearly not the case and has led Mühlford et al. to suggest that this slower rise is due to intramolecular vibrational redistribution and relaxation.<sup>27</sup> The time scale for this seems rather slow, but this is clearly a possibility, although one might anticipate spectral shifts as for solvent relaxation. Our conclusion, as stated earlier, is that the transient spectrum contains contributions from two different excited tautomer species, which are possibly in (rapid) equilibrium with each other given the decay times of a few nanoseconds that are observed at all wavelengths across the transient absorption spectrum.<sup>28</sup> We are currently analyzing further data on femto-second pump–probe studies of 4'-substituted 3-hydroxyflavones, and we will return to the question of the origin of the picosecond transient in a later paper.

**Acknowledgment.** We thank the University of Central Lancashire for a research studentship (SA-B) and BNFL plc for financial support. We thank the EPSRC for granting us access to the Central Laser Facility at the Rutherford Appleton Laboratory and the European Union for support under the "Access to Large-Scale Facilities" program, which enabled us to undertake experimental work at the Max-Born-Institut in Berlin (project # MBI-97-008-01) and LENS (contract # ERBFMGECT950017).

## References and Notes

- Ormsom, S. M.; Brown, R. G. *Prog. React. Kinet.* **1994**, *19*, 45.
- LeGourrierec, D.; Ormsom, S. M.; Brown, R. G. *Prog. React. Kinet.* **1994**, *19*, 211.
- Lärmer, F.; Elsaesser, T.; Kaiser, W. *Chem. Phys. Lett.* **1988**, *148*, 119.
- Elsaesser, T.; Lärmer, F.; Frey, W. *Inst. Phys. Conf. Ser.* **1991**, *126*, 543.
- Wiechmann, M.; Port, H.; Lärmer, F.; Frey, W.; Elsaesser, T. *Chem. Phys. Lett.* **1990**, *165*, 28.
- Chudoba, C.; Lutgen, S.; Jentzsch, T.; Riedle, E.; Wörner, M.; Elsaesser, T. *Chem. Phys. Lett.* **1995**, *240*, 35.
- Chudoba, C.; Riedle, E.; Pfeiffer, M.; Elsaesser, T. *Chem. Phys. Lett.* **1996**, *263*, 622.
- Zhang, H.; van der Meulen, P.; Glasbeek, M. *Chem. Phys. Lett.* **1996**, *253*, 97.
- Marks, D.; Zhang, H.; Glasbeek, M.; Borowicz, P.; Grabowska, A. *Chem. Phys. Lett.* **1997**, *275*, 370.
- Marks, D.; Zhang, H.; Glasbeek, M. *J. Lumin.* **1998**, *76 & 77*, 52.
- Neuwahl, F. V. R.; Foggi, P.; Brown, R. G. *Chem. Phys. Lett.* **2000**, *319*, 157.
- Sekikawa, T.; Kobayashi, T.; Inabe, T. *J. Phys. Chem. A* **1997**, *101*, 644.
- Kobayashi, T.; Sekikawa, T.; Inabe, T. *J. Lumin.* **1997**, *72–74*, 508.
- Mitra, S.; Tamai, N. *Chem. Phys. Lett.* **1998**, *282*, 391.
- Herek, J. L.; Pedersen, S.; Bañares, L.; Zewail, A. H. *J. Chem. Phys.* **1997**, *97*, 9046.
- Sengupta, P. K.; Kasha, M. *Chem. Phys. Lett.* **1979**, *68*, 382.
- Itoh, M.; Tokumura, K.; Tanimoto, Y.; Okada, Y.; Takeuchi, H.; Obi, K.; Tanaka, I. *J. Am. Chem. Soc.* **1982**, *104*, 4146.
- Brucker, G. A.; Kelley, D. F.; Swinney, T. C. *J. Phys. Chem.* **1991**, *95*, 3190.
- Sarkar, M.; Sengupta, P. K. *Chem. Phys. Lett.* **1991**, *179*, 68.
- McMorrow, D.; Kasha, M. *J. Am. Chem. Soc.* **1983**, *105*, 5133.
- McMorrow, D.; Kasha, M. *J. Phys. Chem.* **1984**, *88*, 2235.
- McMorrow, D.; Dzugas, T. P.; Aartsma, T. J. *Chem. Phys. Lett.* **1984**, *103*, 492.
- Brucker, G. A.; Kelley, D. F. *J. Phys. Chem.* **1988**, *92*, 3805.
- Ernsting, N. P.; Dick, B. *J. Chem. Phys.* **1989**, *136*, 181.
- Dzugas, T. P.; Schmidt, J.; Aartsma, T. J. *Chem. Phys. Lett.* **1986**, *127*, 336.
- Rullière, C.; Déclemey, A. *Chem. Phys. Lett.* **1987**, *134*, 64.
- Schwartz, B. J.; Peteanu, L. A.; Harris, C. B. *J. Phys. Chem.* **1992**, *96*, 3591.
- Mühlford, A.; Bultmann, T.; Ernsting, N. P.; Dick, B. In *Femtosecond Reaction Dynamics*; Wiersma, D. A., Ed.; Royal Netherlands Academy of Arts and Sciences: Amsterdam, 1993; p 83.
- Ormsom, S. M.; LeGourrierec, D.; Brown, R. G.; Foggi, P. *J. Chem. Soc. Chem. Commun.* **1995**, 2133.
- Smith, M. A.; Neumann, R. M.; Webb, R. A. *J. Heterocyclic Chem.* **1968**, *5*, 425.
- Velapoldi, R. A.; Mielenz, K. D. *NBS Special Publication 260-64*; National Bureau of Standards: Washington, DC, 1980.
- O'Connor, D. V.; Phillips, D. *Time-correlated Single Photon Counting*; Academic Press: London, 1984.
- Brown, R. G. In *Environmental Photochemistry*, Boule, P., Ed.; Springer: Berlin, 1998; p.27.
- Sparrow, R.; Brown, R. G.; Evans, E. H.; Shaw, D. *J. Chem. Soc., Faraday Trans. 2* **1986**, *82*, 2249.
- Matousek, P.; Parker, A.; Taday, P.; Toner, W.; Towrie, M. *Opt. Commun.* **1996**, *127*, 307.
- Stingl, A.; Lenzner, M.; Spielmann, C.; Krausz, F.; Szipocs, R. *Opt. Lett.* **1995**, *20*, 604.
- Duhr, O.; Nibbering, E. T. J.; Korn, G. *Appl. Phys. B* **1998**, *67*, 525.
- Nibbering, E. T. J.; Duhr, O.; Korn, G. *Opt. Lett.* **1997**, *22*, 1335.
- Bayanov, I. M.; Danielius, R.; Heinz, P.; Seilmeier *Opt. Commun.* **1994**, *113*, 99.
- Danielius, R.; Piskarskas, A.; Di Trapani, P.; Sndreoni, A.; Solcia, C.; Foggi, P. *Appl. Opt.* **1996**, *35*, 5336.
- Ormsom, S. M.; Brown, R. G.; Vollmer, F.; Rettig, W. *J. Photochem. Photobiol. A: Chem.* **1994**, *81*, 65.
- Itoh, M.; Fujiwara, Y. *Chem. Phys. Lett.* **1986**, *130*, 365.
- Pfeiffer, M.; Lau, A.; Lenz, K.; Elsaesser, T. *Chem. Phys. Lett.* **1997**, *268*, 258.